Dynamic Response of Carbon Nanotube Field Effect Transistor Circuits

Yau Xu and Ashok Srivastava*

Department of Electrical and Computer Engineering
Louisiana State University, Baton Rouge, LA, USA 70803-5901
*Phone: (225) 578-5622; Fax: (225) 578-5200; E-mail: ashok@ece.lsu.edu

ABSTRACT

In this work, a current transport equation of CNT-FET is used to describe static characteristics. Dynamic characteristics are obtained from Meyer capacitance model of the CNT-FET. The Verilog-AMS language supports transistor behavior description and is used for the circuit simulations. In addition, a CNT interconnect model is described and combined with the CNT-FET current transport model to study the dynamic response of integrated CNT-FET circuits, such as the inverter pair and ring oscillator.

Keywords: carbon nanotubes, CNT-FET modeling, CNT interconnect, nanotechnology.

1 INTRODUCTION

A good amount of work on modeling carbon nanotube field-effect transistors (CNT-FETs) has been reported [1-4]. However, these models are still numerical-based and require a mathematical/software realization. Recently, Marulanda, Srivastava and Sharma [5] have obtained an analytical solution of current transport model for the CNT-FET for analysis and design of CNT-FET based integrated circuits. Based on their work, a dynamic model for CNT-FETs is obtained and Verilog-AMS language [6] used to predict static and dynamic characteristics of CNT-FETs and integrated circuits.

Fetter [7, 8] and Maffucci et al., [9] have investigated electron transport along the CNT and proposed a two-dimensional fluid model. In this model [7-9], electron-electron correlation, which is significant in CNT, has not been considered. Therefore, we have made modification in two-dimensional fluid model to include electron-electron repulsive interaction and built a semi-classical one-dimensional fluid model [10], which is relatively easy to solve and apply in CNT transmission line modeling.

2 CNT-FET MODEL

1.1 Static model

Current equations are given in [5] which are described here as follows and includes both drift current and diffusion currents.

$$\begin{aligned} I_{ds} &= I_{drift} + I_{diff} \\ &= \beta\left[f_{drift}\left\{\Psi_{cnt,s}(L), V_{gs}\right\} - f_{drift}\left\{\Psi_{cnt,s}(0), V_{gs}\right\}\right] + \\ &+ \beta\left[f_{diff}\left\{\Psi_{cnt,s}(L), V_{gs}\right\} - f_{diff}\left\{\Psi_{cnt,s}(0), V_{gs}\right\}\right] \end{aligned} \quad (1)$$

where

$$f_{drift}\left(\psi_{cnt,s}(x), V_{gs}\right) = \left(V_{gs} + V_{sb} - V_{fb}\right)\psi_{cnt,s}(x) - \frac{1}{2}\psi_{cnt,s}^2(x)$$

$$f_{diff}\left(\psi_{cnt}(x), V_{gs}\right) = \frac{kT}{q}\psi_{cnt,s}(x)$$

$$\beta = \gamma\frac{\mu C_{ox1}}{L^2}$$

In Eq. (1), various parameters are defined as follows: L: gate length, μ: carrier mobility, k: Boltzmann constant, T: temperature, ^{o}K, V_{fb}: flat-band voltage, V_{gs}: gate-source voltage, V_{sb}: source-substrate voltage, $\psi_{cnt,s}$: surface potential of CNT, C_{ox1}: gate-oxide capacitance per unit area. For a carbon nanotube of length L and radius r in a CNT-FET, the oxide capacitance is given by [11],

$$C_{ox1} = 2\pi\varepsilon_{ox1}L \Big/ \ln\left(\frac{T_{ox1} + r + \sqrt{T_{ox1}^2 + 2T_{ox1}r}}{r}\right) \quad (2)$$

1.2 Dynamic Model

To model dynamic response of CNT-FETs, we have used a Meyer capacitance model [12-14]. In a recent work [14], we have obtained capacitances, C_{gs}, C_{gd} and C_{gb} based on current transport modeling of CNT-FETs described by Eq. (1), which are as follows:
In linear region:

$$C_{gb} = 0 \quad (3a)$$

$$C_{gs} = -\frac{\mu W|C_h|C_{ox1}^2}{\beta} \cdot \frac{\left[\delta Ie^{-1} - \delta\Delta(\phi_0 - \frac{\Delta E_F}{q} + \frac{E_c}{q} - \frac{kT}{q} + V_{fb} - V_{gs})\right]\left[\delta Ie^{-1} - \delta\Delta(\phi_0 - \frac{\Delta E_F}{q} + \frac{E_c}{q} - \frac{kT}{q} + V_{fb} - \frac{2}{3}V_{gd} - \frac{1}{3}V_{gs})\right]}{\left[\delta Ie^{-1} - \delta\Delta(\phi_0 - \frac{\Delta E_F}{q} + \frac{E_c}{q} - \frac{kT}{q} + V_{fb} - \frac{1}{2}V_{gd} - \frac{1}{2}V_{gs})\right]^2} \quad (3b)$$

$$C_{gd} = -\frac{\mu W|C_h|C_{ox1}^2}{\beta} \cdot \frac{\left[\delta Ie^{-1} - \delta\Delta(\phi_0 - \frac{\Delta E_c}{q} + \frac{E_c}{q} - \frac{kT}{q} + V_{fb} - V_{gs})\right]\left[\delta Ie^{-1} - \delta\Delta(\phi_0 - \frac{\Delta E_c}{q} + \frac{E_c}{q} - \frac{kT}{q} + V_{fb} - \frac{1}{3}V_{gd} - \frac{2}{3}V_{gs})\right]}{\left[\delta Ie^{-1} - \delta\Delta(\phi_0 - \frac{\Delta E_F}{q} + \frac{E_c}{q} - \frac{kT}{q} + V_{fb} - \frac{1}{2}V_{gd} - \frac{1}{2}V_{gs})\right]^2} \quad (3c)$$

In saturation region:

$$C_{gb} = 0 \tag{4a}$$

$$C_{gs} = \frac{2}{3}\frac{\mu W |C_h| C'^2_{ox1}}{\beta} \tag{4b}$$

$$C_{gd} = 0 \tag{4c}$$

Considering C_{sb} and C_{db} to be equal to one half the insulator capacitance, $C_{ox2}/2$ in series with the depletion-layer capacitance, $C_{subs}/2$ [15, 16], we obtain,

$$C_{ox2} = 2\pi\varepsilon_{ox2} L \Big/ \ln\left(\frac{T_{ox1} + r + \sqrt{T_{ox2}^2 + 2T_{ox2} r}}{r}\right) \tag{5}$$

$$C_{subs} = \frac{N_A q\varepsilon_s + \sqrt{N_A q\varepsilon_s}\sqrt{8C_{ox2}^2 V_{gb} + N_A q\varepsilon_s - 8C_{ox2}^2\phi_{ms} - 8C_{ox2}^2\psi_{cnt}}}{4C_{ox2}\left(V_{gb} - \phi_{ms} - \psi_{cnt}\right)} \tag{6}$$

where ε_s is the permittivity of the semiconductor, W_s is the depletion region width and N_A is the doping concentration.

3 CNT INTERCONNET MODEL

Based on two-dimensional fluid model developed by Maffucci et al., [9] we have proposed one-dimensional fluid model to describe the electron transport in metallic CNT and built a transmission line model of metallic CNT interconnects [10]. The basic equation is as follows,

$$mn_0\frac{\partial v_z}{\partial t} = -\frac{\partial \delta p}{\partial z} - en_0\{(1-\alpha)\boldsymbol{\mathcal{E}}_z\} - mn\{\mathrm{sgn}(l)\}\upsilon v_z \tag{7}$$

where n_0 is the equilibrium electron density, v is the electron mean velocity, p is the pressure, m is the electron mass, e is the electronic charge and $\boldsymbol{\mathcal{E}}_z$ is electric field. The last term on the right hand side represents the effect of scattering of electrons with the positive charge background and υ is the electron relaxation frequency, $\upsilon = v_F/\lambda$ and λ is the mean-free path of electron in CNT. Length of CNT is l and $sgn(l)$ is the sign function defined as follows, $\mathrm{sgn}(l) = \begin{cases} 0 & \text{if} \quad l < 1\mu m \\ 1 & \text{if} \quad l \geq 1\mu m \end{cases}$. The parameter, α describes the classical electron-electron repulsive interaction [10],

The equation relating current density, charge density and electric field can be described as follows [10],

$$\frac{\partial j(z,t)}{\partial t} + \upsilon j + u_e^2\frac{\partial \sigma(z,t)}{\partial z} = \frac{e^2 n_0}{m}(1+\alpha)\boldsymbol{\mathcal{E}}_z \tag{8}$$

We consider a metallic single-walled CNT above a perfect conducting plane and assume [9] that the propagating EM wave is in quasi-TEM mode [9]. The voltage and current intensity are then expressed as follows,

$$i(z,t) = \oint \vec{j}\cdot\vec{z}dl \approx 2\pi r j(z,t) \tag{9}$$

$$q(z,t) = \oint \vec{\sigma}\cdot dl \approx 2\pi r\sigma(z,t) \tag{10}$$

Following the work of Maffucci et al, [9], we combine Eqs. (9), (10) and (8) and obtain,

$$\boldsymbol{\mathcal{E}}_z = Ri + L_K\frac{\partial i}{\partial t} + \frac{1}{C_Q}\frac{\partial q}{\partial z} \tag{11}$$

where $R \equiv L_K\,\mathrm{sgn}(l)\nu$ is the resistance of CNT, $L_K \equiv m/\left[(1+\alpha)2\pi r e^2 n_0\right]$ is the kinetic inductance and $C_Q \equiv 1/L_K u_e^2$ is quantum capacitance per unit length.

The magnetic inductance and electric capacitance per unit length of a perfect conductor on ground plane are given by [17],

$$L_M = \frac{\mu}{2\pi}\cosh^{-1}\left(\frac{h}{r}\right) \approx \frac{\mu}{2\pi}\ln\left(\frac{h}{2r}\right) \tag{12}$$

$$C_E = \frac{2\pi\varepsilon}{\cosh^{-1}(h/r)} \approx \frac{2\pi\varepsilon}{\ln(h/r)} \tag{13}$$

where h is the distance of CNT to the ground plane. Equations (12) and (13) are accurate enough for $h>2r$.

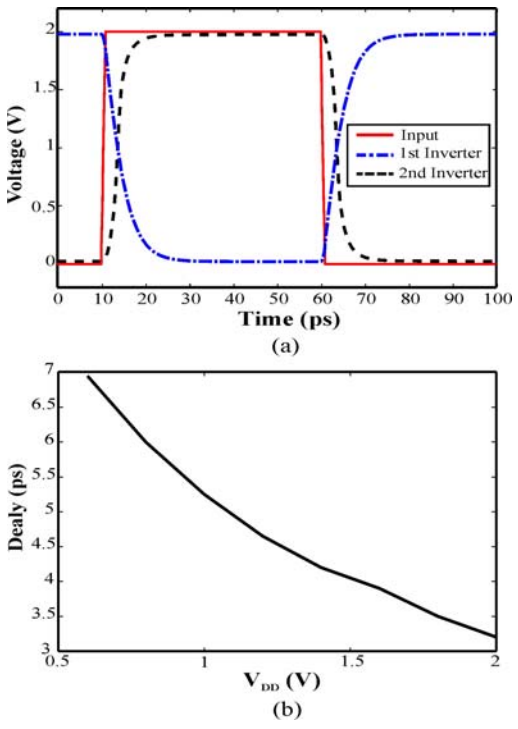

Figure 1: (a) Voltage transfer characteristics of an inverter pair using CNT-FETs (11,9) with $V_{fb} = 0$ *V* and $\Phi_0 = 0$. The dimensions of both the n-type CNT-FET and p-type CNT-FET are: $T_{ox1} = 15$ *nm*, $T_{ox2} = 120$ nm and $L = 250$ *nm*. (b) Average delay of the inverter pair versus supply voltage.

NSTI-Nanotech 2009, www.nsti.org, ISBN 978-1-4398-1782-7 Vol. 1, 2009

4 CIRCUITS SIMULATION

We have used Verilog-AMS language to model CNT-FETs using model equations described in Section 2. Static and dynamic performances are then studied in Cadence/Spectre.

Figure 1(a) shows the signal response of an inverter pair. The input signal is a *10 GHz* square wave. The simulation results show that the delay of the inverter pair is about *3.2 ps*. Figure 1(b) shows a plot of the inverter pair average delay versus the supply voltages. At *0.6 V* supply voltage, the average delay is *6.95 ps*, which suggests that the inverter pair can respond to *100 GHz* input signal.

To study the CNT interconnection delay, we have simulated the inverter pair with CNT wire interconnecting the output and input of the first and second inverter. Figure 2 shows the delay versus the length of CNT interconnection at *2 V* power supply. The longer the interconnection the more delay it gives.

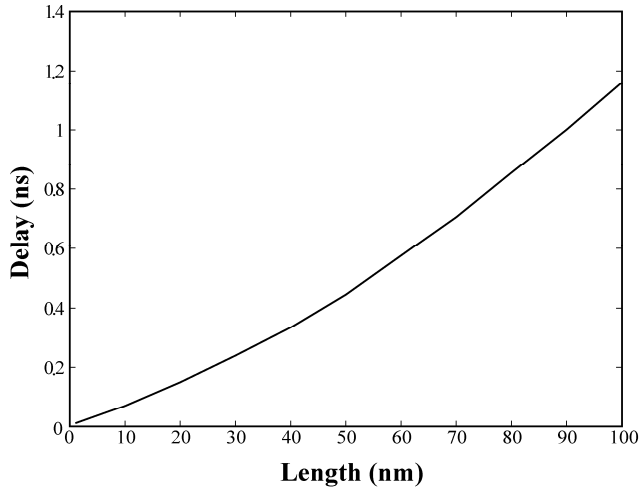

Figure 2: Inverter pair delay versus CNT interconnection length.

Figure 3 (a) shows the schematic of a five stage ring oscillator circuit which was fabricated by Chen et al, [18]. Figure 3 (b) shows the simulation result of the ring oscillator output waveform at 0.92 V supply voltage. Figure 3 (c) shows the oscillation frequency with varying supply voltage. The modeled curve does not include effects of channel length modulation. The experimental data are taken from the work of Chen et al., [18]. Modeled and experimental curves show that the frequency of the ring oscillator is about *70-80 MHz* at *1.04 V* supply voltage. This is because CNT-FETs in this ring oscillator are *600 nm* long and there are parasitic capacitances associated with the metal wire in the ring oscillator. Figure 4 shows frequency dependence of ring oscillator on CNT wire interconnect lengths connecting output to input. As shown in Fig. 4, longer the interconnect wire length is, lower the frequency is of the ring oscillator.

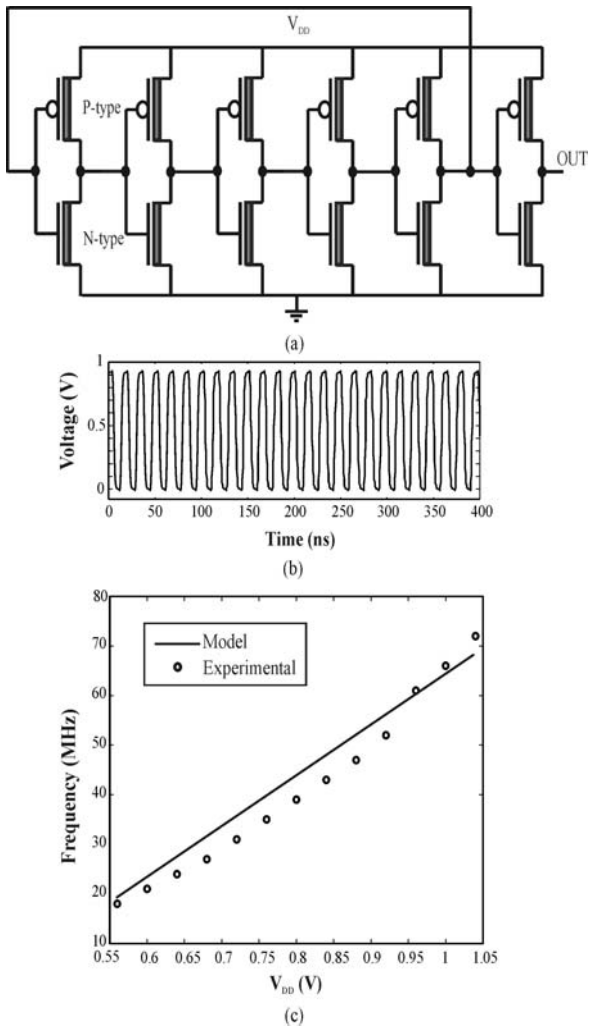

Figure 3: (a) schematic of a 5-stage ring oscillator, (b) output waveform of the ring oscillator and (c) oscillating frequency versus supply voltage, V_{DD}. Dimensions of both the n- and p-type CNT-FETs are: d = 2 nm and L = 600 nm.

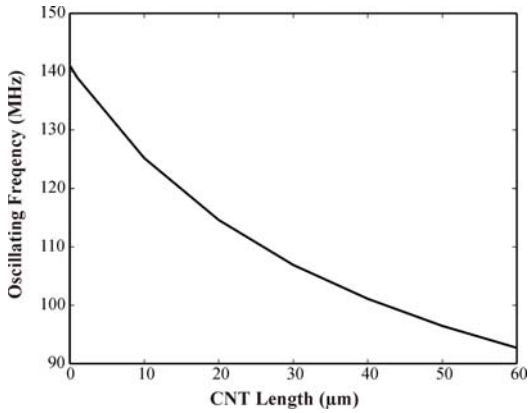

Figure 4: Oscillating frequency of a 5-stage ring oscillator versus length of the CNT interconnects.

5 CONCLUTION

Cadence/Spectre simulations using our models for CNT and CNT-FETs show that carbon nanotube based integrated circuits can perform at very high frequencies and CNT interconnect can be used in CNT-FET integrated circuits.

ACKNOWLEDGMENT

The authors acknowledge the support provided by the Louisiana Economic Development Assistantship (EDA) program to carry out the proposed research. In part the work is also supported under Contract NSF (2009)-PFUND-138 and United States Air Force Contract No. FA9401-08-P-0129. Authors also acknowledge many useful discussions with Dr. Ashwani K. Sharma of U.S. Air Force Research Laboratory, KAFB, NM.

REFERENCES

[1] F. Nihey, H. Hongo, Y. Ochiai, M. Yudasaka, and S. Iijima, "Carbon-nanotube field effect transistors with very high intrinsic transconductance," Jpn. J. Appl. Phys., vol. 42, pp. L1288-L1291, Oct. 8 2003.

[2] S. J. Wind, J. Appenzeller, R. Martel, V. Derycke, and P. Avouris, "Vertical scaling of carbon nanotube field-effect transistors using top gate electrodes," Applied Physics Letters, vol. 80, pp. 3817-3819, May 20 2002.

[3] J. W. Park, J. B. Choi, and K. H. Yoo, "Formation of a quantum dot in a single-walled carbon nanotube using the Al top-gates," Applied Physics Letters, vol. 81, pp. 2644-2646, Sep. 30 2002.

[4] F. Nihey, H. Hongo, M. Yudasaka, and S. Iijima, "A top-gate carbon – nanotube field-effect transistor with a titanium-dioxide insulator," Jpn. J. Appl. Phys., vol. 41, pp. L1049-L1051, Oct. 2002.

[5] J. M. Marulanda, A. Srivastava, and A. K. Sharma, "Current transport modeling in carbon nanotube field effect transistors (CNT-FETs) and bio-sensing applications," in Proc. SPIE: Nanosensors and Microsensors for Bio-Systems, vol. 6931, pp. 693108-12, 2008.

[6] "Verilog-AMS Language Reference Manual," http://www.designers-guide.org/VerilogAMS/, August 2008.

[7] A. L. Fetter, "Electrodynamics of a layered electron gas. I. single layer," Annals of Physics, vol. 81, pp. 367-393, 1973.

[8] A. L. Fetter, "Electrodynamics of a layered electron gas. II. periodic array," Annals of Physics, vol. 88, pp. 1-25, 1974.

[9] A. Maffucci, G. Miano, and F. Villone, "A transmission line model for metallic carbon nanotube interconnects," Int. J. Circuit Theory Appl., vol. 36, pp. 31-51, 2008.

[10] Y. Xu and A. Srivastava, "A Model for Carbon Nanotube interconnects," Int. J. Circ. Theor. Appl., Accepted, 2009.

[11] D. T. Thomas, "Engineering Electromagnetics," Pergamon Press, 1972.

[12] T. A. Fjeldly, T. Ytterdal, and M. S. Shur, "Introduction to Device Modeling and Circuit Simulation," Wiley, 1998.

[13] Y. Cheng and C. Hu, "MOSFET Modeling and BSIM3 User's Guide," Springer, 1999.

[14] Y. Xu and A. Srivastava, "Transient Behavior of Integrated Carbon Nanotube Field Effect Transistor Circuits," in Proc. SPIE: Nano-, Bio, and Info-Tech Sensors and Systems, vol. 7291, 2009 (in press).

[15] B. Streetman and S. Banerjee, "Solid State Electronic Devices," 5th ed. Upper Saddle River, New Jersey: Prentice Hall, 2000.

[16] S. J. Wind, J. Appenzeller, R. Martel, V. Derycke, and P. Avouris, "Fabrication and electrical characterization of top gate single-wall carbon nanotube field-effect transistors," J. Vac. Sci. Technol. B, vol. 20, pp. 2798-2801, Nov. 2002.

[17] S. Ramo, J. R. Whinnery, and T. V. Duzer, "Fields and Waves in Communication Electronics." New York: Wiley, 1994.

[18] Z. Chen, J. Appenzeller, P. M. Solomon, Y.-M. Lin, and P. Avouris, "High performance carbon nanotube ring oscillator," the 64th Device Research Conference, 2006, State College, PA, USA, 2006, pp. 171-172.